Heliyon 7 (2021) e06652

Contents lists available at ScienceDirect

Heliyon

journal homepage: www.cell.com/heliyon

Research article

Magnetic polymeric core-shell as a carrier for gradual release in-vitro test drug delivery

Maryam Zhalechin [a], Shahram Moradi Dehaghi [a,*], Mostafa Najafi [b], Abolghasem Moghimi [a]

[a] Department of Chemistry, Tehran North Branch, Islamic Azad University, Tehran, Iran
[b] Department of Chemistry, Faculty of Science, Imam Hossein University, Tehran, Iran

ARTICLE INFO

Keywords:
Nanotechnology
Pharmaceutical chemistry
Core-shell
Nilotinib
Gradual release
Magnetic
Graphene oxide
Drug delivery

ABSTRACT

At first functionalized graphene oxide was selected as a basic substrate obtained through process of functionalization of graphene oxide with *diethylenetriamine* as substrates. Then magnetic nanoparticle sediments were formed and coated on the functionalized graphene oxide as the core center. The core nanoparticle was added to a gel containing poly (lactic-co-glycolic acid), polyethylene glycol, and polyvinylpyrrolidone and nilotinib drug for forming a shell on the core. After separation and freeze-drying, single core-shell particles were obtained. The second shell was coated by dispersing first core-shell in a new gel containing polylactic acid, polyvinyl alcohol, polyethylene glycol, and nilotinib. The third layer was laminated on core-dual shell particle by entering in sodium alginate, polyethylene glycol, poly (lactic-co-glycolic acid), polylactic acid and nilotinib gel according to the same method used above. In order to determine the gradual release, the core-single, dual and triple shell nanoparticles dispersed in phosphate buffer saline at the several pHs (3, 5.4, 7.4) and as well as monitoring the released concentration of nilotinib by UV-Vis spectrophotometer technique. Core-triple shell particle had gradual release at three different rates over the long time. Finally, the average release rate for 400 mg of drug, in single layer, double-layer and three layers were reported to be equal to 15.8, 10.4 and 6.6 mg/h at intervals of 24, 37 and 60 h, respectively. The release rate of the drug reduced by increasing the pH value. All products were characterized using several techniques.

1. Introduction

Nowadays, the core-shell particles have been applied for smart drug delivery. Different methods and materials have been used for preparation of core-shell nanoparticles. The synergistic effect, loading capacity, power of influence, biocompatibility, biodegradability, dissolution, and stability environment all were considered to be the determinant parameters in the construction of core-shell composites [1, 2, 3]. In recent years, the core-shell composites have been used in different cases including smart drug delivery, bio imaging, sensing, replacement, support, tissues, catalysis and electronics. Biocompatible polymers used in the preparation of core-shell composites for drug delivery and making pharmaceutical carriers are of interest to researchers [2, 4].

Core-shell particles were prepared usually by two methods including two-step or multi-step process methods. In these methods, initially, the core particles were synthesized and the shell was formed on the core particle using different methods, such as sol-gel, hydrolysis and hydrothermal [1, 2, 4].

The hollow shell, rattle-like, yolk shell, Nano porous core-shell all were different types of core-shell [4]. Core-shell and some of the organic and inorganic polymers have been used for the preparation microspheres [5, 6, 7, 8, 9, 10, 11]. Core-shell in medication applications has been used for drug delivery of nilotinib (Figure 1) [12,13,14], Doxorubicin [15, 16], 5-Flu [17, 18] and other drugs in the treatment of cancer and other diseases [19].

In this study, the core-shell was produced by deposition of super paramagnetic particles onto graphene oxide functionalized with diethylenetriamine. This composite was milled to fine spherical particles using a disk mill. After separation and drying, the spherical particles were introduced into a gel containing multiple biodegradable natural polymers. Then, a certain amount of nilotinib was added to the mixture. The gel was milled by the disk mill until the core-shell nanostructures were obtained. Multiple single-layered structures owning different percentages of polymer and drug were obtained. Drug releasement for all three types of nanoparticles, including core-shell particles (CSP), core-dual shell particles (CDSP) and core-triple shell particles (CTSP) was

* Corresponding author.
E-mail address: shm_moradi@iau-tnb.ac.ir (S.M. Dehaghi).

https://doi.org/10.1016/j.heliyon.2021.e06652
Received 23 June 2019; Received in revised form 7 September 2019; Accepted 1 October 2019

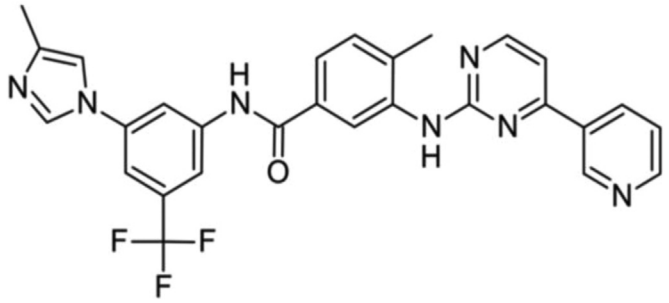

Figure 1. Nilotinib drug structure as a sample test.

evaluated in the phosphate buffer saline environment at 37 °C and three pHs (3, 5.4, 7.4) [20,21,22]. Different single-layered structures were prepared using polymer structural parameters including polymerization degree, hydrolysis degree, and molecular mass. It was found that the release time differed based on the properties of the employed polymers. The solubility of the polymers reduced and the release time increased when the molecular mass and polymerization degree were increased. Ultimately, core-dual and core-triple nanostructures were prepared based on the results obtained from single-layered core-shell nanostructures. Also, release time and proportional release rate for an extended period were obtained based on the results.

2. Experimental

2.1. Materials

The major reagents used in this research were as follows: Graphene Oxide was purchased from Shanghai Yifan Graphite Co., Ltd.; Diethylene Triamine, Oxalyl Chloride, Dimethyl Formamid (DMF), Tetra Hydro Furan (THF), Ferric Chloride hexahydrate (FeCl3,6H2O, 99%), anhydrous Dimethyl Sulfoxide (DMSO), Acetic Acid, Sulphuric Acid, Phosphate Buffered Saline (PBS) and Nilotinib, were purchased from Sigma Aldrich Co.; Polyvinylpyrrolidone (PVP, K30) was purchased from MYM Biological Technology Co., Ltd. poly (lactic-co-glycolic acid (PLGA), Polylactic acid (PLA), Na Alginate and Glycerol monostearate (GMS), Polyethylene glycol (PEG) were purchased from Sigma Aldrich Co.

2.2. Synthesis method

2.2.1. Preparation of functionalized graphene oxide (FGO)

Graphene oxide was converted into chloroacetic acid form through the reaction with oxalyl chloride. Chloroacetic acid form of graphene oxide reacted with diethylenetriamine under the influence of microwave irradiations based on the procedure presented in the study by Moradi [23]. The method was as follows.

2.2.2. Acylation of graphene oxide (G-COCl)

0.1 g of GO was dispersed in 60 mL of Dimethylformamide (DMF) by the sonication treatment for 15 min. Next, 8 mL of oxalyl chloride was added drop wise to the dispersion of GO at 0 °C under nitrogen gas and the mixture was stirred at 0 °C for 2h and then was kept at room temperature for 2h. The excess oxalyl chloride was removed by heating the reaction mixture at 70 °C for 12 h the G-COCl was collected by filtration through a membrane (pore size of 0.2 μm) and was dried under vacuum.

2.2.3. Amidation of chloroacetic acid form of graphene oxide

0.1 g of G-COCl was heated with 0.05 mol of DMF at 100 °C for 7 days, separately. After being washed with ethanol to remove the excess amine, the black solid was treated with Tetrahydrofuran (THF). The brownish mixture was filtered through a coarse filter paper and the black filtrate was taken to be dried in a rotary evaporator.

2.2.4. Synthesis of magnetic FGO (MFGO)

The method presented in the reference was modified [24, 25, 26, 27], to synthesize and stabilize iron magnetic nanoparticles on FGO. Initially, FGO was dissolved in aqueous solution and a solution of $FeCl_3$ and $FeCl_2$ with a 2:1 M ratio was added to it. Then, 1.0 M of trimethyl ammonium hydroxide was prepared and was added slowly to the solution until the pH of the solution reached about 12. The solution was sonicated for 20 min then was stirred for 3 h to be homogenized. Then, MFGO particles were separated using a permanent magnet from suspension and were washed several times with deionized water and were dried in an oven at around 60 °C for 48 h under vacuum. The samples were then pressurized using an abrasive stirrer to form spherical particles as well as achieving better interactions between FGO and magnetic nanoparticles. Functionalized graphene oxide coated with magnetic nanoparticles, MFGO was prepared according to this method, as shown in Figure 2.

2.2.5. Preparation of core-shell, core -double shell and core-triple shell nano particles

In the production process, at first, the single-layered core-shell nanostructures were prepared. The preparation procedure was the same except some parameters such as molecular mass and polymerization degree. The preparation process is brought in Table 1. It describes the type and properties of utilized polymers in the production of single layered core-shells in order to the optimization of used polymers ratios.

As shown in Figure 2, MFGO was used as a core for the preparation of core-shell composite. MFGO was added to the hydro-alcoholic gel

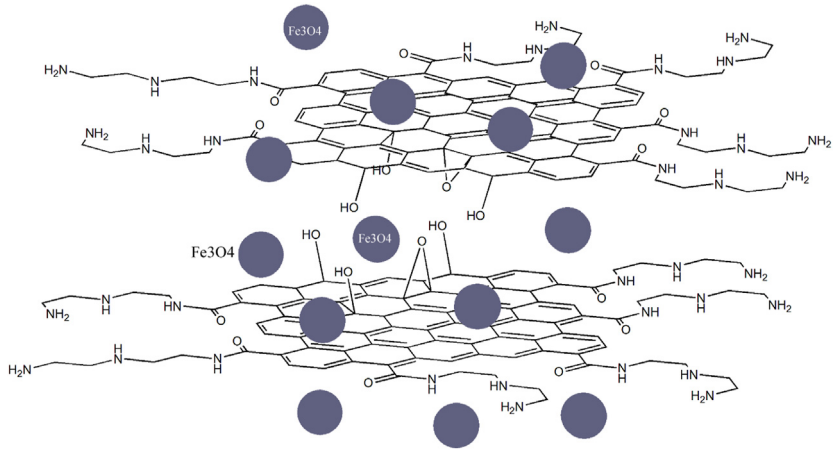

Figure 2. The central structure forms core in the core-shell composite.

containing Polyvinylpyrrolidone (PVP) and polyethylene glycol (PEG) and nilotinib drug. The poly lactic-co-glycolic acid (PLGA) was dissolved in chloroform and was added to an insignificant amount of glycerin mono stearate (GMS) as an emulsifier. After mixing the whole pellet containing the resulting mixture, the gel was added in the first step. The mixture was stirred until the solvent was evaporated and the gel was coated on functionalized graphene oxide nano particles (FGONP), and the mixture was tightly mixed by an abrasive stirrer to fit uniformly, so that the mixture can be crossed completely and easily from sieve with mesh 800, then was diluted with double distilled water. The mixture was quickly sprayed onto liquid nitrogen and remained for 1 h for complete freezing. The frozen nanoparticles were transferred to a petri dish and it was lyophilized (freeze-dryer bone (FDB-5503), Operon. company) for 5 days in order to dry the first nano particles. The CSP were prepared. Then, again, a part of CDSP was added to the new hydro-alcoholic gel containing PEG and PVP and a new dose of the nilotinib drug at 0°c was mixed with polylactic acid (PLA) solution in chloroform and was added to an in significant amount of glycerin mono-stearate as an emulsifier. The mixture was stirred and the second layer was laminated to be placed on CDSP. According to the same method used for the preparation of the first core-shell nano particles, CDSP was dried and separated. In the third step, again, some of the CDSP were added to another hydro-alcoholic gel containing hydroxy propyl cellulose (HPC), PEG, Na alginate, PLGA, PLA and was mixed with the other dose of the nilotinib drug according to the same method. The final gel was added to the calcium chloride solution, was stirred gently for 2 h. The resulting paste was shaken and tiny particles were sieved. The mixture was prepared according to the same method before lyophilization. CTSP were prepared. The image of the core and the structure of multi-layer core-shell particles are presented in Figure 3.

Nilotinib drug values in CSP were 0.4 g. In CDSP, added nilotinib drug mass amounts were 0.2 g in the inner shell and 0.2g in the outer layers. Nilotinib drug amounts in CTSP from inside to outside of the shells were 0.1, 0.15 and 0.15 g, respectively.

2.3. Drug release

Drug release in phosphate buffered saline (PBS) was investigated at pH values of 3, 5.4 and 7.4 and the temperature at 37 °C. The drug release for CSP, CDSP and CTSP in the above conditions was evaluated separately. The amount of drug released during a specific time was measured by UV-Vis spectroscopy. Table 1 shows the drug release in various conditions. Table 1 and Graph 1 provide the rate and process of drug release for all core-shell nano particles.

3. Results and discussion

3.1. Characterization

The results of the FT-IR (Thermo Nicolet Nexus 870 FT-IR spectroscopy) to determine the functional groups, ^{1}H NMR, ^{13}C NMR (Fourier transform Nuclear Magnetic Resonance (FT-NMR) Bruker, 300 MHz) To determine the structure of functionalized graphene oxide, Vibrating Sample Magnetometer (VSM, Homade 2 T) In order to investigate the magnetic properties of iron oxide nanoparticles, Scanning Electron Microscopy (SEM, XL30, 15–30 KV, Philips Company Electron Microscopes) in order to evaluate the morphology of the surface of the core-shell, Transmission Electron Microscopy (TEM,CM 30, 300 KV) to study the core-shell particle size, Thermogravimetric Analysis TGA (LINSEIS

Table 1. Provides the rate and drug releases process for all core-shell.

		Loaded drug (mg/g)	Released drug (mg)	Average rate of released (mg/h)	Duration time (h)	% Released
pH ~ 3.0						
CSP		**400**	**380**	**15.8**	**~24**	**95**
CDSP	Outer shell	200	198	11.64	~17	99
	Inner shell	200	192	9.6	~20	96
Total		**400**	**390**	**~ 10.4**	**~ 37**	**97.5**
CTSP	Outer shell	150	150	8.33	~18	100
	Middle shell	150	148	6.72	~22	98.6
	Inner shell	100	98	4.9	~20	98
Total		**400**	**396**	**~ 6.6**	**~ 60**	**99**
pH ~ 5.4						
CSP		**400**	**340**	**8.5**	**~ 40**	**85**
CDSP	Outer shell	200	190	7.0	**~ 27**	95
	Inner shell	200	185	7.4	**~ 25**	92.5
Total		**400**	**375**	**~ 7.2**	**~ 52**	**93.75**
CTSP	Outer shell	150	150	6.8	**~22**	100
	Middle shell	150	147	5.65	**~26**	98
	Inner shell	100	90	4.0	**~24**	90
Total		**400**	**387**	**~ 5.4**	**~72**	**96.75**
pH ~ 7.4						
CSP		**400**	**320**	**6.6**	**~48**	**80**
CDSP	Out shell	200	170	6.1	~28	85
	Inner shell	200	150	5.0	**~30**	75
Total		**400**	**320**	**~5.5**	**~58**	**80**
CTSP	Out shell	150	145	5.0	**~28**	96
	Middle shell	150	140	4.0	**~35**	93
	Inner shell	100	75	2.5	**~30**	75
Total		**400**	**360**	**~3.9**	**~93**	**90**

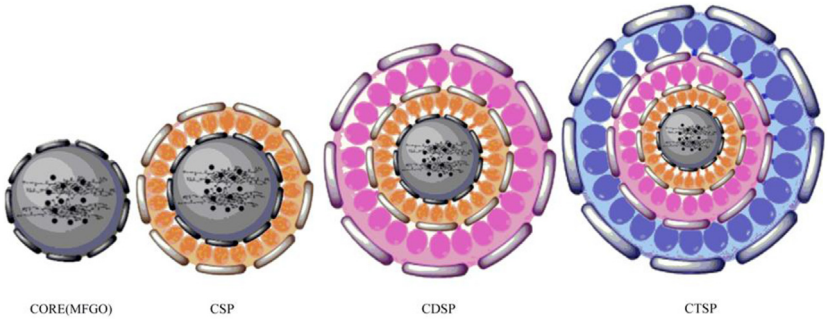

Figure 3. The image of the core and the structure of multi-layer core-shell composites.

Thermal Analysis STA PT 1600) were presented separately for each product, which is as follows:

3.2. FT-IR

At the end of each stage of the process including the production of magnetic nanoparticles, functionalization of graphene oxide with diethylenetriamine and nilotinib, and production of CSP, CDSP and CTSP, and FT-IR spectroscopy was implemented for all the samples. Stretching vibrational (SV) and bending vibrational (BV) frequency range of functional groups in the compounds were presented and described below (Figure 4).

Stretching vibration of N–H and NH2 groups of diethylene tri-amine and the functional amine group of Nilotinib in the range of 3400–3580 cm-1 can be seen. Carbonyl functional group stretching vibrations in the amide group are observed in the functionalized graphene oxide in the core and nilotinib drug structure in the range of 1610–1710 cm-1. Other significant signals of functional groups for the ingredients in core-shells, respectively, are presented below.

FGO: ν_{max} (KBr disc): 3470 s (NH, NH_2) (SV); 1710w (C=O) (SV); 1610 m (CONH) (SV); 1090 w (C–N) (BV), cm^{-1}.;/(s: strong, m: medium, w: weak); **MFGO**: ν_{max} (KBr disc): 3580 s (NH, NH_2) (SV); 1700 s (C=O), 630 (Fe_3O_4) (BV), cm^{-1}; **CSP**: ν_{max} (KBr disc): 3400s (NH, NH_2) (SV); 1610s (CO) (SV); 640w (Fe_3O_4) (BV); cm^{-1}. **CDSP**: ν_{max} (KBr disc): 3400s, (NH, NH_2) (SV); 1610s, (C=O) (SV); 1420m, (Fe_3O_4) (BV); 670w, (NH) (BV), cm^{-1}. **CTSP**: ν_{max} (KBr disc): 3400s, (NH, NH_2) (SV); 1610s, (C=O) (SV); 1420m, (Fe_3O_4) (BV); 670w, (NH) (BV), cm^{-1}.

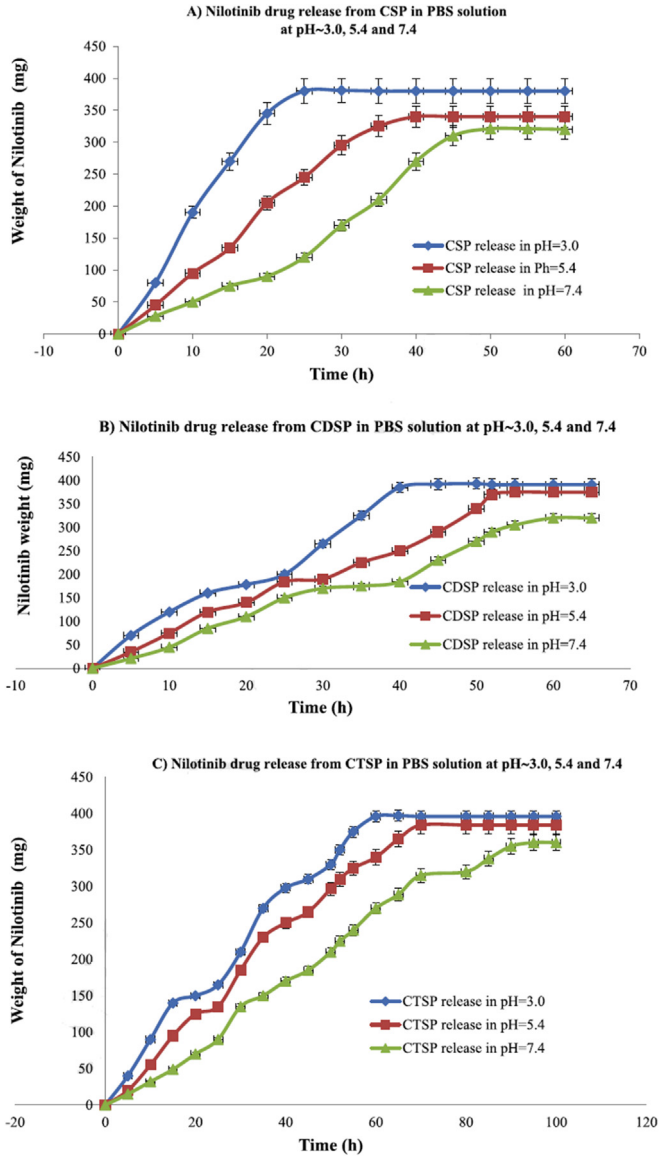

Graph 1. Nilotinib drug release from SCP(A), CDSP(B), CTSP(C) in PBS solution at pH~3.

3.3. NMR

Figure 5 shows the MFGO spectral specification represented by determining the functional groups and their chemical shift in the ^{13}C and ^{1}H-NMR spectrum. Since the oxidation process differed from the graphene sheets, it's completely different functional groups position and is non-uniform. The functional groups on graphene oxide structure are non-repeatability. In the functionalization spectrum obtained is decentralized and dispersed in a close range together. For this reason, broad peaks were observed extensively. Diethylenetriamine, amide group created after attaching it to graphene. NH groups of di-ethylenetramine was existed in two form, amine and amide group and due to the hydrogen bonding in ^{1}H NMR was observed in the range of 8–9 ppm with broad singlet peak that is exchanged hydrogen with D_2O. Methylene hydrogens that connected to the amine and amide groups in ^{1}H NMR and the appearing of methylene carbon in the ^{13}C NMR is expressed, respectively.

^{1}H NMR ($CDCl_3$ solution): δ 8–9 s (N**H**) broad singlet exchange D_2O; 5–4.3, m (CO–NH– C**H$_2$**); 3.0–3.4, m (C**H$_2$**–NH); ppm. ^{13}C {^{1}H} NMR ($CDCl_3$ solution): δ 170 (**C**=O); 163, 161 (**C**, GO); 57 (CO–N–**C**H_2); 30–41 (NH–**C**H_2); ppm.

3.4. SEM and TEM images

The first row of Figure 6 shows the SEM images for all samples in which the spherical structure was confirmed and the average particle size for the MFGO, CSP, CDSP and CTSP core-shell was determined to be equal to 60, 110, 230 and 330 nm, respectively.

Second row of Figure 6 shows the results obtained from the TEM images, with a high similarity ratio, in which the spherical structure of the shell-core nano particle was confirmed and the average particle size for MFGO, CSP, CDSP and CTSP was determined to be equal to 65, 110,

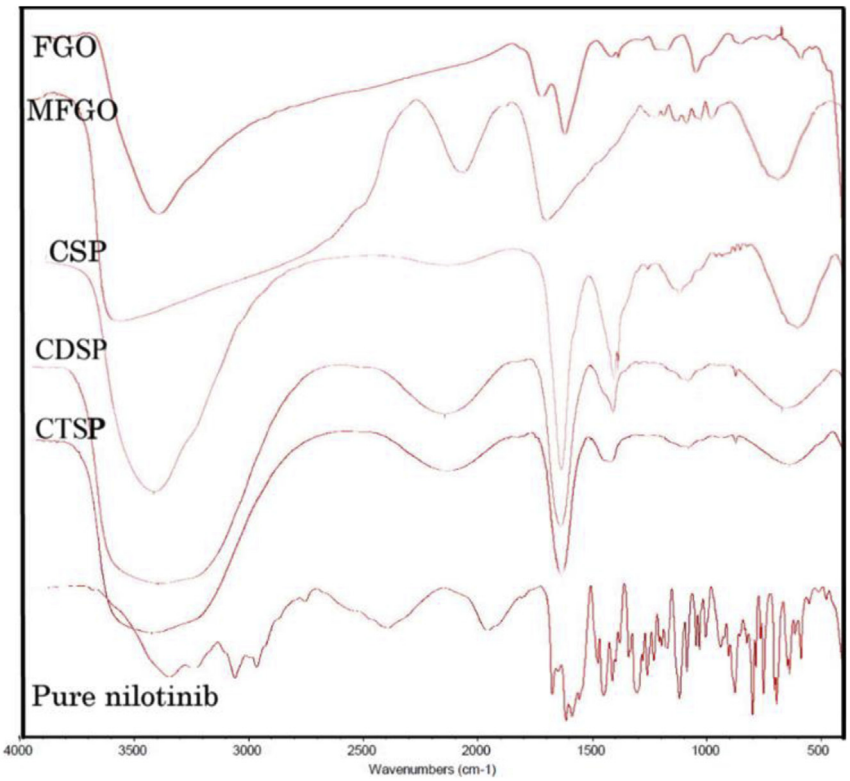

Figure 4. The image of the FT-IR spectrum.

222 and 325 nm, respectively. The layered structure in the core shell particles was clearly visible in the TEM images. The increase in the size of the particle by increasing each layer on the substrate was easily recognizable.

3.5. Vibrating sample magnetometer

Figure 7 shows the Vibrating Sample Magnetometer (VSM) images, according to VSM results, the magnetic properties of MFGO particles showed the maximum saturation magnetization which was equal to 40.1emu/g indicating a typical super paramagnetic behavior. By placing the first shell on the core, the magnetic properties are reduced, with the second and third layers reaching 37.5, 30.0 and 26.8emu/g, respectively. The amount of magnetic nanoparticles in the core is fixed. Padding is done on the same core. With increasing each layer on the core, the ratio of magnetic mass in core is reduced to the total mass of core-shell nanoparticles. The loss of the magnetic properties due to reduction mass of the magnetic core compared to the total mass of core-shell nanoparticles.

3.6. TGA thermogram interpretation

Figure 8 shows the Thermogravimetric analysis (TGA) thermogram, the results of Thermogravimetric Analysis for CTSP show that there are layers decomposing along with a slowly increasing temperature. The weight loss of about 30% for sodium alginate was observed at a temperature of 180–250 °C [28]. A thermal degradation was observed for the PLGA at the temperature range of 250–320 °C in which the composite weight decreased about 11% The composite weight decreased by 11% due to the weight loss of the PLA at the temperature range of 320–370 °C [29, 30].

The next weight loss was observed at the temperature range of 370 up to 400 °C and 400 up to 470, which is attributed to the weight loss of PVAl was and it was reported to be about 10% of the composite weight and PVP about 10% [31, 32]. Weight loss associated with the nilotinib and diethylenetriamin at the temperature range of 470 up to 620 °C, it was reported to be about 16% of the composite weight. Weight loss associated with the graphene oxide continued to the temperature of 700 °C, it was reported to be about 10% of the total composite weight less than 2% of the composite weight remained constant and was not changed with the change in the temperature, which belonged to the magnetic iron oxide present in the composite sample.

4. Discussion

The experience we obtained in the process of pro duction of nanoparticles can be represented as follows. At first, the magnetic nanoparticles were added to the mixture of drug and polymer without the functionalized graphene oxide support. In this case, the structure did not own the core, and also the magnetic charges of the nanoparticles were distributed all over the nanoparticles due to scatteredness of magnetic nanoparticles in the solution. Therefore, the effect of external magnetic field on the concentration of the drug was insignificant. In the next stage, the magnetic nanoparticles were loaded on FGO support. The presence of amine groups and their interaction with iron salts in the production stage induced the precipitation of magnetic nanoparticles within the FGO layers and formation of strong intermolecular forces. This process caused more concentration of magnetic nanoparticles. Also using the disk mill/mixer made the particles to become more spherical and dense. These particles were significantly attracted to the magnetic field due to their high concentration and density. The noticeable point is that these particles collapsed partially in further stages. Moreover, increasing the number of layers on the core reduced the magnetic effect due to the reduction of the ratio of core magnetic mass to the whole particle mass.

The results showed that, CTSP compared to CDSP have a lower average release rate and a longer period was reported for the release. In these samples, the drug used was the same in all nano medicines and the dose of the drug was equal to 400 mg. According to the results, the drug

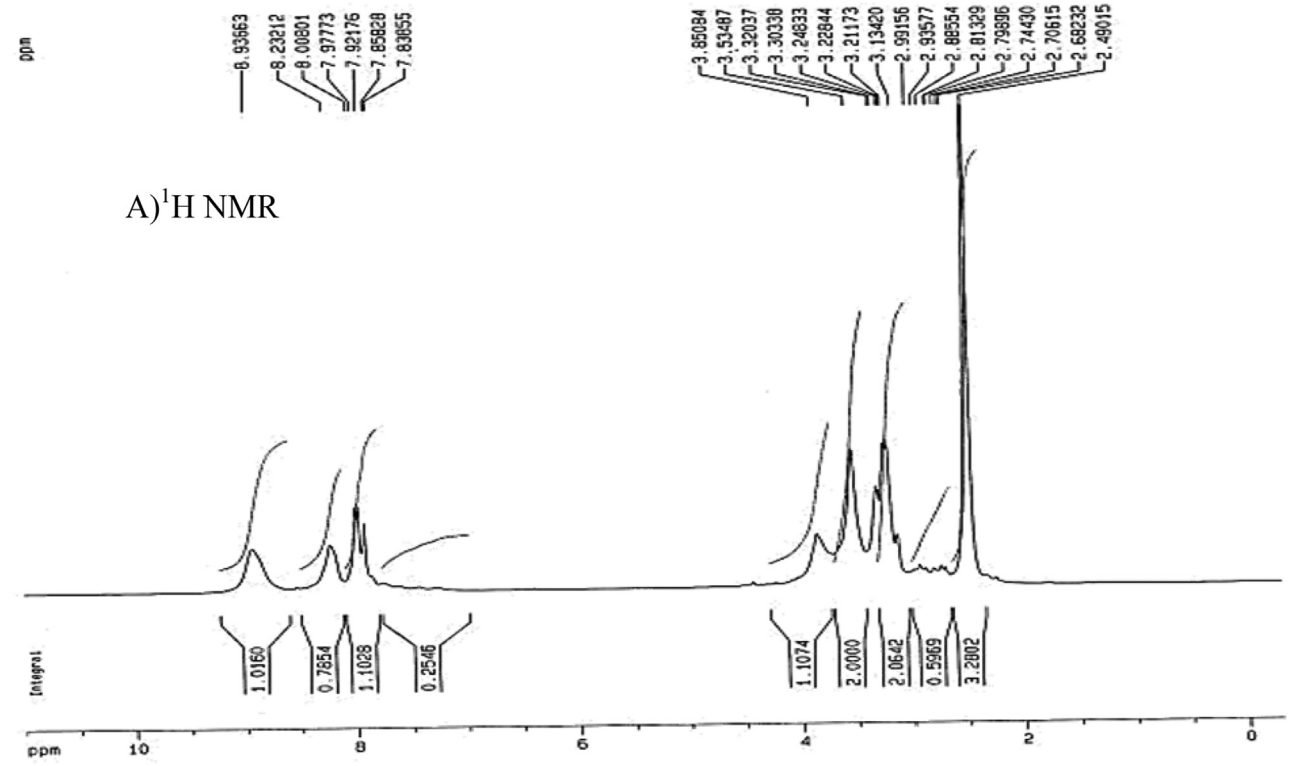

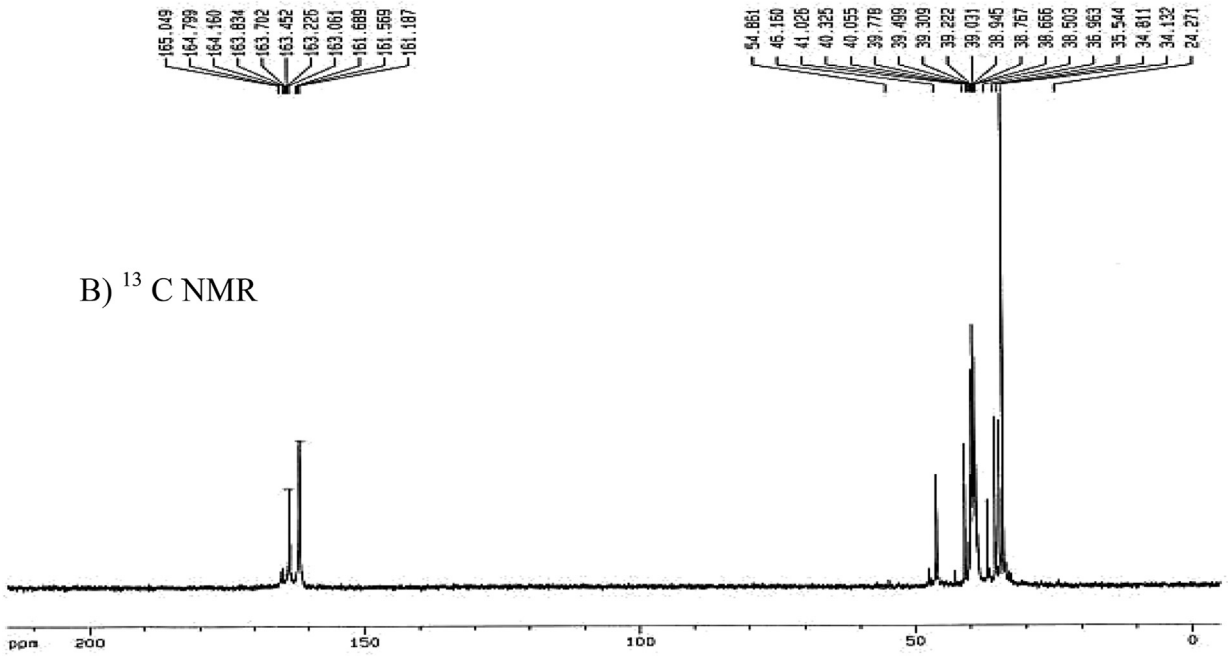

Figure 5. ^{1}H NMR(A) and ^{13}C NMR(B) images for all the spherical structure MFGO.

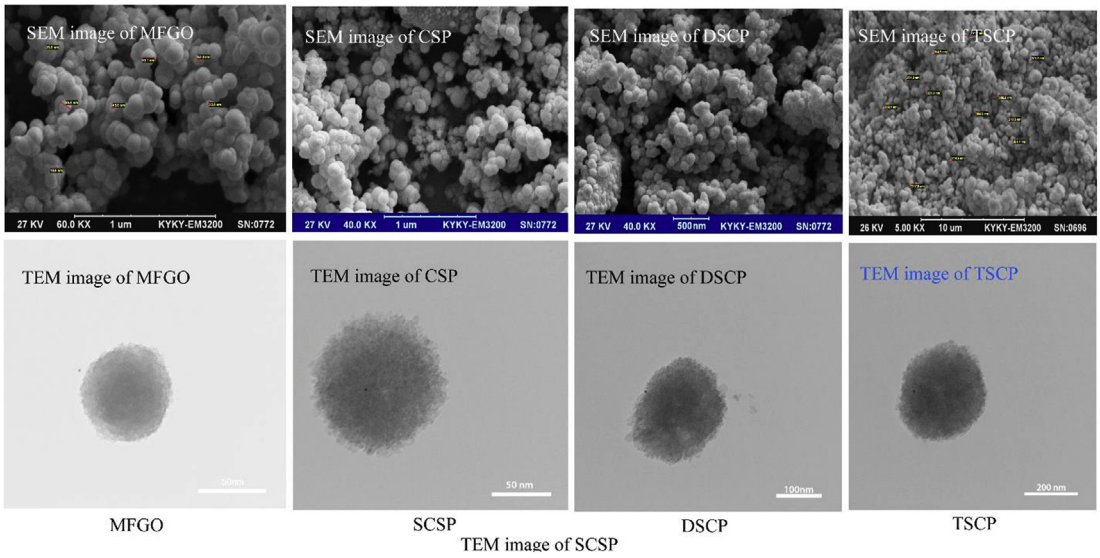

Figure 6. The above figure is related to SEM and the bottom image is TEM for all the spherical structure MFGO, CSP, CDSP, and CTSP.

loaded in the CDSP showed 48-hour efficiency from 98% to 93 h compared to 99% efficiency for TSCP, while its release rate dropped from 6.6 to 3.9 mg/h, respectively.

Through the acidification of PBS, its release rate increases in all samples. Table 1 compares the drug release rate in different values of pHs. The drug release behavior was nearly linear when nearly 50% of the weight of the nanoparticle was loaded with drugs, but by increasing levels of drug more than this amount, its release rate increased.

The experience gained in the manufacturing of nano medicines showed that using natural polymers for drug delivery can be achieved in a fit and healthy condition. Based on the experience in this study, it was found that by increasing molecular weight of PLGA and PLA, dissolution rate decreased and delivery time increased.

Finally, with the same molecular weight of PLGA and PLA, the appropriate interaction between the dissolution and the drug loading was established.

The use of auxiliary polymers such as Polyvinyl alcohol (PVAl), and PVP led to an appropriate dispersion of medication at the time of mixing with PLGA and PLA to create a proper distribution.

By increasing the number of shells, the amount of drug loading increased in each of the nanoparticles, and by determining the type of polymer and its degree of polymerization, its release rate can be controlled.

In addition, different drugs can be loaded simultaneously or in different shells. By increasing the number of shells to a thickness of 5,000 nm, a significant amount of the drug can be released in a long time.

Finally, in this study, the nilotinib drug was loaded into shells of core-shell nanoparticles containing one to three shells. The environmental conditions were investigated for drug release in the stomach environment with pH~ 3.4, in the cancer cellular environment with pH~ 5.4 and also in neutral environments with pH~7.4 in the PBS environment. In fact, these three pHs have direct contact with the iso-electric point of

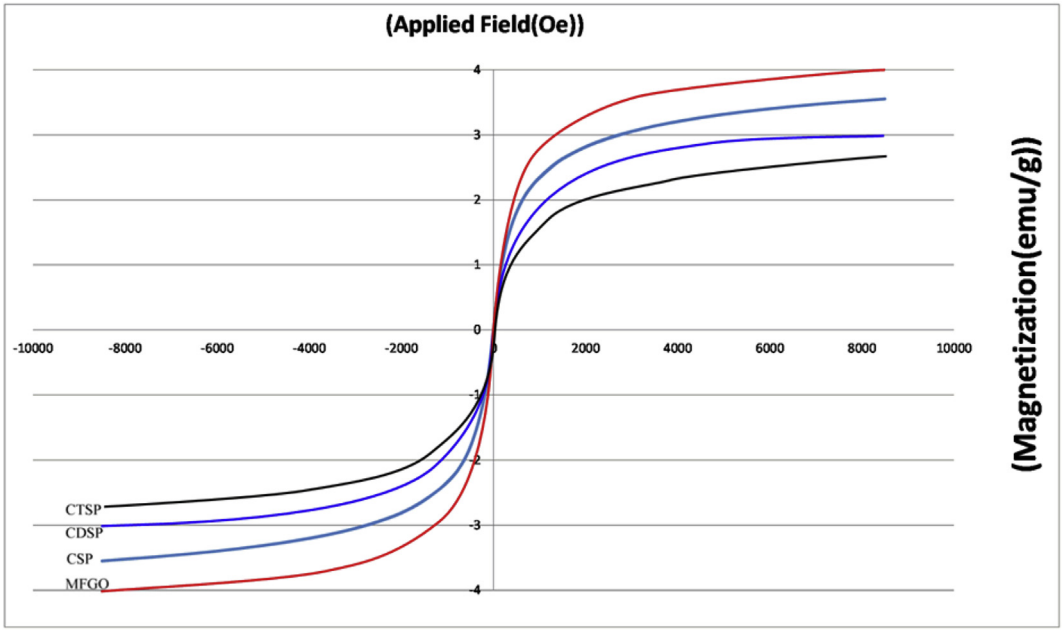

Figure 7. The VSM images related to magnetic properties of MFGO particles.

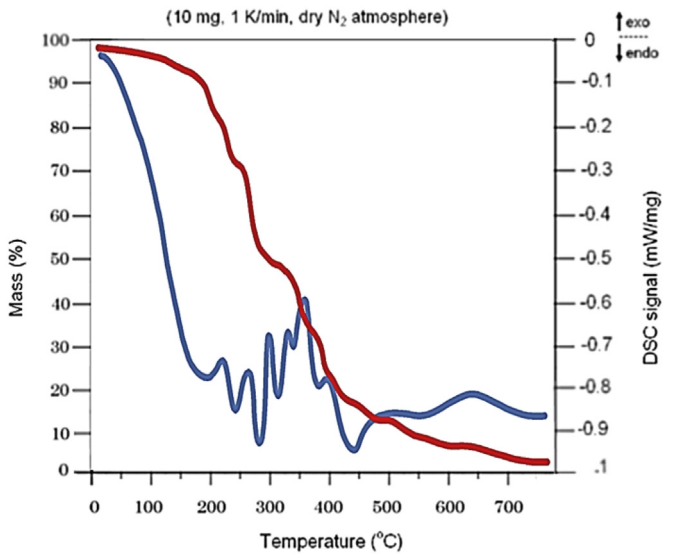

Figure 8. The Thermal gravimetric analysis and Differential thermal analysis (TGA-DTA) of the CTSP.

protein and amino acids, in acidic, neutral and alkaline of the body's physiological environment. The amount of drug was equal in three samples.

In normal conditions, due to the very low dissolution of the drug in body's physiological environments, high amounts of medicine are injected into the body. Nilotinib drug is very harmful for the body, additionally, large quantities of medicine are removed through sweating, urine and stool from the body. Due to the high cost for this drug, its release control and slowing down the process of drug release is considered necessary, while it can lead to the reduction of the potential for long-term absorption and reduction of drug intake, as well as reduction of injuries.

Therefore, the mechanism of drug replacement has been achieved with a specific amount in the short and long term. A distinctive feature used to slow down the release of insoluble drugs such as nilotinib was noted in the body's physiological environment. It is usually prescribed with high doses, which only a slight amount is absorbed into the body and the rest of it is excreted. Super magnetic particles were embedded in the core-shell. An external magnetic field was used to focus its release on the damaged site. Super magnetic particles are activated and absorbed into the magnetic field. This feature can be employed for preventing scatteredness of the drug and concentrating it in the desired spot. However, such a process would have more utilization in clinical trials, but in this study, it was measured as a single parameter.

Finally, after the release of the drug, the external magnetic field is removed; the remaining material is excreted from the body. Polymer used in preparation of the core -shell, was biocompatible and did not cause any problems for the body. The goal of this study was to prepare the drug carriers. The remarkable point is that the carrier can be used to transfer any other medicines or substances in the body.

5. Conclusion

Generally, it is worthy to say that in this study, the possibility of loading and slow releasement of nilotinib drug was evaluated through finding the proper mess proportion of biocompatible polymers of PLA and PLGA. Some of the valuable results were obtained during the process, and some beneficial modifications were applied as follows.

- Production of magnetic nanoparticles on FGO support in order to obtain higher concentration and more magnetic attraction between magnetic nanoparticles and FGO was implemented. These properties prevented scatteredness and lack of concentration of the particles which keep them from being attracted to the external magnetic field.
- We employed disk mills in order to production and compression of magnetic and core-shell nanoparticles somehow that the densest nanoparticles with high range of grain size are obtained. These properties were achieved through a change in the pressure of the mill disks.
- Finding the correlation between the molecular mass of the polymers and their mixture ratios was implemented in order to achieve the desired releasement time. Increasing the molecular mass of poor soluble polymers such as PLA and PLGA (molecular mass from 33000 to 55000 and 88000) in PBS environment allows us to extend the releasement time. On the other hand, in the case of PVAl, increasing the hydrolysis degree of acetate groups in PVAl up to 98% promoted the formation of hydrogen bonding in the mentioned molecule. This phenomenon enhanced the formation of a low-soluble and sturdy polymer film which helped to slow down the releasement process.
- The role of PVP and GMS as emulsifiers were considerable since PVP, PVAl, and the drug are produced in water and alcohol environment, while PLA and PLGA are produced in chloroform. PVP and GAAS facilitated the interactions between those two phases and promoted the formation of some tiny but stable micelles which dispersed the particles and homogenized the mixture well.
- We used numerous samples to find the optimized mixture ratio.
- Using sodium alginate in the outer shell had some tangible benefits as it aided well formation of the outer shell and the spherical growth of the core-shell. As soon as the final mixture was homogenized, the gel was introduced into the disk mill which was placed in calcium chloride solution. Then, the particles rapidly started to gain spherical shapes. As a matter of fact, sodium alginate has a significant ability to absorb water. This improves a facilitated dissolution with the absorption of water and more drug releasement from the outer shell. In other words, the drug releasement rate in a sodium alginate support is extremely higher than PLA and PLGA. Adding sodium alginate is for the releasement in the first moments. Drug releasement from the outer shell in the samples without sodium alginate was nearly zero in some hours.
- The mass amount of nilotinib drug (400 mg) and the super paramagnetic particles (0.01 g) and total MFGO mass (0.1 g) was constant in all the samples. In multi-layered samples, the sum of drug mass in each layer was 400 g. The change in the polymer types and their mass ratio are adjusted based on the drug releasement time. This change is depended on the solubility in PBS, so certain amounts of drugs can be released in a long time. As the last point to mention, nilotinib is a cancer drug, therefore its releasement behavior was evaluated in 3 common pHs in the body.
- This release rate in the acidic medium in CSP was on average 15.8 mg/h for 24 h. For CDSP, the average release rate was equal to 10.4 mg/h for 37 h and for CTSP average release rate was equal to 6.6 mg/h for 60 h. Based on the results and the experience gained in the construction of core-shell nanoparticles, it was found that they can be used for two or more drugs at the same time. Each layer can be assigned to a single drug. By increasing the size of the nanoparticles the drug load percentage can be increased.
- About CSP, the releasement rate increased when the pH reduced. 400 mg of nilotinib in pH of 7.4 had 48 h of releasement time, in pH of 5.4 it was 40 h, and in pH of 3, it was 24 h. About CDSP, the releasement time of 400 mg of nilotinib in three pH of 7.4, 5.4, and 3 was 58, 52, and 37 respectively. About CTSP and the same pHs, the releasement time was 93, 72, and 60 h respectively.

Declarations

Author contribution statement

Shahram Moradi Dehaghi: Conceived and designed the experiments; Analyzed and interpreted the data; Contributed reagents, materials, analysis tools or data; Wrote the paper.

Maryam Zhalechin: Performed the experiments; Analyzed and interpreted the data.

Mostafa Najafi: Conceived and designed the experiments; Analyzed and interpreted the data; Contributed reagents, materials, analysis tools or data.

Abolghasem Moghimi: Analyzed and interpreted the data; Contributed reagents, materials, analysis tools or data.

Funding statement

This research did not receive any specific grant from funding agencies in the public, commercial, or not-for-profit sectors.

Competing interest statement

The authors declare no conflict of interest.

Additional information

No additional information is available for this paper.

References

[1] R. Hayes, A. Ahmed, T. Edge, H. Aifei Zhang, Core–shell particles: preparation, fundamentals and applications in high performance liquid chromatography, J. Chromatogr. A 1357 (2014) 36–52.
[2] G. Shim, M.G. Kim, J.Y. Park, Y.K. Oh, Graphene-based nanosheets for delivery of chemotherapeutics and biological drugs, Adv. Drug Deliv. Rev. 105 (2016) 205–227.
[3] K. Yang, L. Feng, Z. Liu, Stimuli responsive drug delivery systems based on nano-graphene for cancer therapy, Adv. Drug Deliv. Rev. 105 (2016) 228–241.
[4] R.G. Chaudhuri, S. Paria, Chem. Rev, Core/shell nanoparticles: classes, properties, synthesis mechanisms, characterization, and applications, Chem. Rev. 112 (2012) 2373–2433.
[5] S.K. Shukla, S.R. Deshpande, S.K. Shukla, A. Tiwari, Fabrication of a tunable glucose biosensor based on zinc oxide/chitosan-graft-poly (vinyl alcohol) core-shell Nano composite, Talanta 99 (2012) 283–287.
[6] M. Wang, D. Fang, N. Wang, S. Jiang, J. Nie, Q. Yu, G. Ma, Preparation of PVDF/PVP coreshell nanofibers mats via homogeneous electrospinning, Polymer 55 (2014) 2188–2196.
[7] I.E. Moreno-Cortez, A. Alvarado-Castañeda, D.F. Garcia-Gutierrez, N.A. Garcia-Gomezc, S. Sepulveda-Guzman, D.I. Garcia-Gutierrez, Core–shell PEDOT: PSS—PVP nanofibers containing PbS nanoparticles through coaxial electrospinning, Synth. Met. 220 (2016) 255–262.
[8] J. Tang, L. Ma, N. Tian, M. Gan, F. Xu, J. Zeng, Y. Tu, Synthesis and electromagnetic properties of PANI/PVP/CIP core–shell composites, Mater. Sci. Eng. B 186 (2014) 26–32.
[9] K. Asadpour-Zeynali, F. Mollarasouli, Novel electrochemical biosensor based on PVP capped $CoFe_2O_4$@CdSe core-shell nanoparticles modified electrode for ultra-trace level determination of rifampicin by square wave adsorptive stripping voltammetry, Biosens. Bioelectron. 92 (2017) 509–516.
[10] C.I. Covaliu, I. Jitaru, G. Paraschiv, et al., Core–shell hybrid nanomaterials based on $CoFe_2O_4$ particles coated with PVP or PEG biopolymers for applications in biomedicine, Powder Technol. 237 (2013) 415–426.
[11] J. Cheng, B.A. Teply, I. Sherifi, et al., Formulation of functionalized PLGA-PEG nanoparticles for in vivo targeted drug delivery, Biomateriala 28 (2008) 869–876.
[12] K. Miyamura, T. Miyamoto, M. Tanimot, et al., Switching to nilotinib in patients with chronic myeloid leukemia in chronic phase with molecular suboptimal response to frontline imatinib: SENSOR final results and BIM polymorphism sub study, Leuk. Res. 51 (2016) 11–18.
[13] M.A. Nader, G.M. Atti, Beneficial effects of nilotinib, tyrosine kinase inhibitor on cyclosporine-A induced renal damage in rats, Int. Immunopharm. 33 (2016) 1–7.
[14] M. Crampe, J. Garry, S.E. Langabeer, et al., Sustained molecular response with nilotinib in imatinib-intolerant chronic myeloid leukaemia with an e19a2 BCR-ABL1 fusion, Hematol. Oncol. Stem Cell Ther. 9 (2016) 168–169.
[15] L.C. Ho, C.H. Hsu, C.M. Ou, et al., Unibody coreshell smart polymer as a theranostic nanoparticle for drug delivery and MR imaging, Biomaterials 37 (2015) 436–446.
[16] L. Liu, J. Zeng, X. Zhao, K. Tian, P. Liu, Independent temperature and pH dual-responsive PMAA/PNIPAM microgels as drug delivery system: effect of swelling behavior of the core and shell materials in fabrication process, Colloid. Surface. Physicochem. Eng. Aspect. 526 (2017) 48–55.
[17] A. Dalmoro, A.Y. Sitenkov, S. Cascone, et al., Hydrophilic drug encapsulation in shell-core microcarriers by two stage polyelectrolyte complexation method, Int. J. Pharm. 518 (2017) 50–58.
[18] D. Liu, D.T. Auguste, Cancer targeted therapeutics: from molecules to drug delivery vehicles, J. Contr. Release 219 (2015) 632–643.
[19] R.A. Perez, H.W. Kim, Core–shell designed scaffolds for drug delivery and tissue engineering, Acta Biomater. 21 (2015) 2–19.
[20] Z. Zhang, R. Zhang, L. Zou, D.J. Mc Clements, Protein encapsulation in alginate hydrogel beads: effect of pH on microgel stability, protein retention and protein release, Food Hydrocolloids 58 (2016) 308–315.
[21] Y. Zhu, J. Shi, Fluoride adsorption from aqueous solution by magnetic core-shell Fe3O4@alginate-La particles fabricated via electro-coextrusion, Microporous Mesoporous Mater. 103 (2007) 243–249.
[22] J. Li, J. Zeng, X. Jia, L. Liu, T. Zhou, P. Liu, pH, temperature and reduction multi-responsive polymeric microspheres as drug delivery system for anti-tumor drug: effect of middle hollow layer between pH and reduction dual-responsive cores and temperature sensitive shells, J. Taiwan Inst. Chem. Eng. (2016) 1–8.
[23] M. Zhalechin, Sh Moradi, P. Abroomand Azar, Synthesis of nano shell by amino functionalization of multi-walled carbon nano tubes, J. Mater. Sci. Eng. 3 (2014) 112–119.
[24] Y. Zhang, X. Lin, Q. Zhou, X. Luo, Fluoride adsorption from aqueous solution by magnetic core-shell Fe_3O_4@alginate-La particles fabricated via electro-coextrusion, Appl. Surf. Sci. 389 (2016) 34–45.
[25] L.P. Lingamdinne, Y.-L. Choi, I.-S. Kim, Y.-Y. Chang, J.R. Koduru, J.-K. Yang, Porous graphene oxide based inverse spinel nickel ferrite nanocomposites for the enhanced adsorption removal of arsenic, RSC Adv. 6 (77) (2016) 73776–73789.
[26] L.P. Lingamdinne, J.R. Koduru, Y.-Y. Chang, R.R. Karri, Process optimization and adsorption modeling of Pb(II) on nickel ferrite-reduced graphene oxide nano-composite, J. Mol. Liq. 250 (2018) 202–211.
[27] L.P. Lingamdinne, J.R. Koduru, R.R. Karri, A comprehensive review of applications of magnetic graphene oxide based nanocomposites for sustainable water purification, J. Environ. Manag. 231 (2019) 622–634.
[28] S. Jana, M.K. Trivedi, R.M. Tallapragada, A. Branton, D. Trivedi, G. Nayak, et al., Characterization of physicochemical and thermal properties of chitosan and sodium alginate after biofield treatment, Pharm. Anal. Acta 6 (2015) 19.
[29] F.S. Marcela, A.W.H. Ana, M.I. Juan, J.A.O. Adilson, A.G.P. Edgardo, Study of Thermal Degradation of PLGA, PLGA Nanospheres and PLGA/Maghemite Super para magnetic Nano spheres, Mater. Res. 18 (6) (2015) 1–20.
[30] S.V.S. Giita, N.A. Ibrahim, W.M. Yunus, H.A. Hassan, C.B. Woei, Comparative study on the mechanical, thermal and morphological characterization of poly(lactic acid)/epoxidized Palm Oil blend1, Int. J. Mol. Sci. 3 (5) (2012) 5878–5898.
[31] W.G. Osiris, T.H.M. Manal, Thermal and structural studies of poly (vinyl alcohol) and hydroxypropyl cellulose blends, Nat. Sci. 4 (1) (2012) 57–67.
[32] J. Sunho, L. Byung-Seok, A. SeJin, H.Y. Kyung, H.S. Yeong, C. Youngmin, H.R. Beyong, Supplementary Information, 8.2% efficient solution-processed $CuInSe_2$ solar cell based on multiphase $CuInSe_2$ nanoparticles, Energy Environ. Sci. 5 (2012) 7539–7542.